Title
Measurement of CP asymmetry in B0→Ks0π0π0 decays

Journal
Physical Review D - Particles, Fields, Gravitation and Cosmology, 76(7)

ISSN
1550-7998

Authors
Aubert, B
Bona, M
Boutigny, D
et al.

Publication Date
2007-10-05

DOI
10.1103/PhysRevD.76.071101

RAPID COMMUNICATIONS

PHYSICAL REVIEW D **76,** 071101(R) (2007)

Measurement of CP asymmetry in $B^0 \rightarrow K_s^0 \pi^0 \pi^0$ decays

B. Aubert,[1] M. Bona,[1] D. Boutigny,[1] Y. Karyotakis,[1] J. P. Lees,[1] V. Poireau,[1] X. Prudent,[1] V. Tisserand,[1] A. Zghiche,[1] E. Grauges,[2] A. Palano,[3] J. C. Chen,[4] N. D. Qi,[4] G. Rong,[4] P. Wang,[4] Y. S. Zhu,[4] G. Eigen,[5] I. Ofte,[5] B. Stugu,[5] G. S. Abrams,[6] M. Battaglia,[6] D. N. Brown,[6] J. Button-Shafer,[6] R. N. Cahn,[6] Y. Groysman,[6] R. G. Jacobsen,[6] J. A. Kadyk,[6] L. T. Kerth,[6] Yu. G. Kolomensky,[6] G. Kukartsev,[6] D. Lopes Pegna,[6] G. Lynch,[6] L. M. Mir,[6] T. J. Orimoto,[6] M. Pripstein,[6] N. A. Roe,[6] M. T. Ronan,[6,*] K. Tackmann,[6] W. A. Wenzel,[6] P. del Amo Sanchez,[7] M. Barrett,[7] T. J. Harrison,[7] A. J. Hart,[7] C. M. Hawkes,[7] A. T. Watson,[7] T. Held,[8] H. Koch,[8] B. Lewandowski,[8] M. Pelizaeus,[8] K. Peters,[8] T. Schroeder,[8] M. Steinke,[8] J. T. Boyd,[9] J. P. Burke,[9] W. N. Cottingham,[9] D. Walker,[9] D. J. Asgeirsson,[10] T. Cuhadar-Donszelmann,[10] B. G. Fulsom,[10] C. Hearty,[10] N. S. Knecht,[10] T. S. Mattison,[10] J. A. McKenna,[10] A. Khan,[11] P. Kyberd,[11] M. Saleem,[11] D. J. Sherwood,[11] L. Teodorescu,[11] V. E. Blinov,[12] A. D. Bukin,[12] V. P. Druzhinin,[12] V. B. Golubev,[12] A. P. Onuchin,[12] S. I. Serednyakov,[12] Yu. I. Skovpen,[12] E. P. Solodov,[12] K. Yu Todyshev,[12] M. Bondioli,[13] M. Bruinsma,[13] M. Chao,[13] S. Curry,[13] I. Eschrich,[13] D. Kirkby,[13] A. J. Lankford,[13] P. Lund,[13] M. Mandelkern,[13] E. C. Martin,[13] D. P. Stoker,[13] S. Abachi,[14] C. Buchanan,[14] S. D. Foulkes,[15] J. W. Gary,[15] F. Liu,[15] O. Long,[15] B. C. Shen,[15] L. Zhang,[15] E. J. Hill,[16] H. P. Paar,[16] S. Rahatlou,[16] V. Sharma,[16] J. W. Berryhill,[17] C. Campagnari,[17] A. Cunha,[17] B. Dahmes,[17] T. M. Hong,[17] D. Kovalskyi,[17] J. D. Richman,[17] T. W. Beck,[18] A. M. Eisner,[18] C. J. Flacco,[18] C. A. Heusch,[18] J. Kroseberg,[18] W. S. Lockman,[18] T. Schalk,[18] B. A. Schumm,[18] A. Seiden,[18] D. C. Williams,[18] M. G. Wilson,[18] L. O. Winstrom,[18] E. Chen,[19] C. H. Cheng,[19] A. Dvoretskii,[19] F. Fang,[19] D. G. Hitlin,[19] I. Narsky,[19] T. Piatenko,[19] F. C. Porter,[19] G. Mancinelli,[20] B. T. Meadows,[20] K. Mishra,[20] M. D. Sokoloff,[20] F. Blanc,[21] P. C. Bloom,[21] S. Chen,[21] W. T. Ford,[21] J. F. Hirschauer,[21] A. Kreisel,[21] M. Nagel,[21] U. Nauenberg,[21] A. Olivas,[21] J. G. Smith,[21] K. A. Ulmer,[21] S. R. Wagner,[21] J. Zhang,[21] A. Chen,[22] E. A. Eckhart,[22] A. Soffer,[22] W. H. Toki,[22] R. J. Wilson,[22] F. Winklmeier,[22] Q. Zeng,[22] D. D. Altenburg,[23] E. Feltresi,[23] A. Hauke,[23] H. Jasper,[23] J. Merkel,[23] A. Petzold,[23] B. Spaan,[23] K. Wacker,[23] T. Brandt,[24] V. Klose,[24] H. M. Lacker,[24] W. F. Mader,[24] R. Nogowski,[24] J. Schubert,[24] K. R. Schubert,[24] R. Schwierz,[24] J. E. Sundermann,[24] A. Volk,[24] D. Bernard,[25] G. R. Bonneaud,[25] E. Latour,[25] Ch. Thiebaux,[25] M. Verderi,[25] P. J. Clark,[26] W. Gradl,[26] F. Muheim,[26] S. Playfer,[26] A. I. Robertson,[26] Y. Xie,[26] M. Andreotti,[27] D. Bettoni,[27] C. Bozzi,[27] R. Calabrese,[27] G. Cibinetto,[27] E. Luppi,[27] M. Negrini,[27] A. Petrella,[27] L. Piemontese,[27] E. Prencipe,[27] F. Anulli,[28] R. Baldini-Ferroli,[28] A. Calcaterra,[28] R. de Sangro,[28] G. Finocchiaro,[28] S. Pacetti,[28] P. Patteri,[28] I. M. Peruzzi,[28,†] M. Piccolo,[28] M. Rama,[28] A. Zallo,[28] A. Buzzo,[29] R. Contri,[29] M. Lo Vetere,[29] M. M. Macri,[29] M. R. Monge,[29] S. Passaggio,[29] C. Patrignani,[29] E. Robutti,[29] A. Santroni,[29] S. Tosi,[29] K. S. Chaisanguanthum,[30] M. Morii,[30] J. Wu,[30] R. S. Dubitzky,[31] J. Marks,[31] S. Schenk,[31] U. Uwer,[31] D. J. Bard,[32] P. D. Dauncey,[32] R. L. Flack,[32] J. A. Nash,[32] M. B. Nikolich,[32] W. Panduro Vazquez,[32] P. K. Behera,[33] X. Chai,[33] M. J. Charles,[33] U. Mallik,[33] N. T. Meyer,[33] V. Ziegler,[33] J. Cochran,[34] H. B. Crawley,[34] L. Dong,[34] V. Eyges,[34] W. T. Meyer,[34] S. Prell,[34] E. I. Rosenberg,[34] A. E. Rubin,[34] A. V. Gritsan,[35] A. G. Denig,[36] M. Fritsch,[36] G. Schott,[36] N. Arnaud,[37] M. Davier,[37] G. Grosdidier,[37] A. Höcker,[37] V. Lepeltier,[37] F. Le Diberder,[37] A. M. Lutz,[37] S. Pruvot,[37] S. Rodier,[37] P. Roudeau,[37] M. H. Schune,[37] J. Serrano,[37] V. Sordini,[37] A. Stocchi,[37] W. F. Wang,[37] G. Wormser,[37] D. J. Lange,[38] D. M. Wright,[38] C. A. Chavez,[39] I. J. Forster,[39] J. R. Fry,[39] E. Gabathuler,[39] R. Gamet,[39] D. E. Hutchcroft,[39] D. J. Payne,[39] K. C. Schofield,[39] C. Touramanis,[39] A. J. Bevan,[40] K. A. George,[40] F. Di Lodovico,[40] W. Menges,[40] R. Sacco,[40] G. Cowan,[41] H. U. Flaecher,[41] D. A. Hopkins,[41] P. S. Jackson,[41] T. R. McMahon,[41] F. Salvatore,[41] A. C. Wren,[41] D. N. Brown,[42] C. L. Davis,[42] J. Allison,[43] N. R. Barlow,[43] R. J. Barlow,[43] Y. M. Chia,[43] C. L. Edgar,[43] G. D. Lafferty,[43] T. J. West,[43] J. I. Yi,[43] C. Chen,[44] W. D. Hulsbergen,[44] A. Jawahery,[44] C. K. Lae,[44] D. A. Roberts,[44] G. Simi,[44] G. Blaylock,[45] C. Dallapiccola,[45] S. S. Hertzbach,[45] X. Li,[45] T. B. Moore,[45] E. Salvati,[45] S. Saremi,[45] R. Cowan,[46] G. Sciolla,[46] S. J. Sekula,[46] M. Spitznagel,[46] F. Taylor,[46] R. K. Yamamoto,[46] H. Kim,[47] S. E. Mclachlin,[47] P. M. Patel,[47] S. H. Robertson,[47] A. Lazzaro,[48] V. Lombardo,[48] F. Palombo,[48] J. M. Bauer,[49] L. Cremaldi,[49] V. Eschenburg,[49] R. Godang,[49] R. Kroeger,[49] D. A. Sanders,[49] D. J. Summers,[49] H. W. Zhao,[49] S. Brunet,[50] D. Côté,[50] M. Simard,[50] P. Taras,[50] F. B. Viaud,[50] H. Nicholson,[51] N. Cavallo,[52,‡] G. De Nardo,[52] F. Fabozzi,[52,‡] C. Gatto,[52] L. Lista,[52] D. Monorchio,[52] P. Paolucci,[52] D. Piccolo,[52] C. Sciacca,[52] M. A. Baak,[53] G. Raven,[53] H. L. Snoek,[53] C. P. Jessop,[54] J. M. LoSecco,[54] G. Benelli,[55] L. A. Corwin,[55] K. K. Gan,[55] K. Honscheid,[55] D. Hufnagel,[55] H. Kagan,[55] R. Kass,[55] J. P. Morris,[55] A. M. Rahimi,[55] J. J. Regensburger,[55] R. Ter-Antonyan,[55] Q. K. Wong,[55] N. L. Blount,[56] J. Brau,[56] R. Frey,[56] O. Igonkina,[56] J. A. Kolb,[56] M. Lu,[56] C. T. Potter,[56] R. Rahmat,[56] N. B. Sinev,[56] D. Strom,[56] J. Strube,[56] E. Torrence,[56] A. Gaz,[57] M. Margoni,[57] M. Morandin,[57] A. Pompili,[57] M. Posocco,[57] M. Rotondo,[57] F. Simonetto,[57] R. Stroili,[57] C. Voci,[57] E. Ben-Haim,[58] H. Briand,[58] J. Chauveau,[58] P. David,[58] L. Del Buono,[58] Ch. de la Vaissière,[58] O. Hamon,[58] B. L. Hartfiel,[58] Ph. Leruste,[58]

1550-7998/2007/76(7)/071101(8)

J. Malclès,[58] J. Ocariz,[58] L. Gladney,[59] M. Biasini,[60] R. Covarelli,[60] C. Angelini,[61] G. Batignani,[61] S. Bettarini,[61] G. Calderini,[61] M. Carpinelli,[61] R. Cenci,[61] F. Forti,[61] M. A. Giorgi,[61] A. Lusiani,[61] G. Marchiori,[61] M. A. Mazur,[61] M. Morganti,[61] N. Neri,[61] E. Paoloni,[61] G. Rizzo,[61] J. J. Walsh,[61] M. Haire,[62] J. Biesiada,[63] P. Elmer,[63] Y. P. Lau,[63] C. Lu,[63] J. Olsen,[63] A. J. S. Smith,[63] A. V. Telnov,[63] F. Bellini,[64] G. Cavoto,[64] A. D'Orazio,[64] D. del Re,[64] E. Di Marco,[64] R. Faccini,[64] F. Ferrarotto,[64] F. Ferroni,[64] M. Gaspero,[64] P. D. Jackson,[64] L. Li Gioi,[64] M. A. Mazzoni,[64] S. Morganti,[64] G. Piredda,[64] F. Polci,[64] C. Voena,[64] M. Ebert,[65] H. Schröder,[65] R. Waldi,[65] T. Adye,[66] G. Castelli,[66] B. Franek,[66] E. O. Olaiya,[66] S. Ricciardi,[66] W. Roethel,[66] F. F. Wilson,[66] R. Aleksan,[67] S. Emery,[67] M. Escalier,[67] A. Gaidot,[67] S. F. Ganzhur,[67] G. Hamel de Monchenault,[67] W. Kozanecki,[67] M. Legendre,[67] G. Vasseur,[67] Ch. Yèche,[67] M. Zito,[67] X. R. Chen,[68] H. Liu,[68] W. Park,[68] M. V. Purohit,[68] J. R. Wilson,[68] M. T. Allen,[69] D. Aston,[69] R. Bartoldus,[69] P. Bechtle,[69] N. Berger,[69] R. Claus,[69] J. P. Coleman,[69] M. R. Convery,[69] J. C. Dingfelder,[69] J. Dorfan,[69] G. P. Dubois-Felsmann,[69] D. Dujmic,[69] W. Dunwoodie,[69] R. C. Field,[69] T. Glanzman,[69] S. J. Gowdy,[69] M. T. Graham,[69] P. Grenier,[69] V. Halyo,[69] C. Hast,[69] T. Hryn'ova,[69] W. R. Innes,[69] M. H. Kelsey,[69] P. Kim,[69] D. W. G. S. Leith,[69] S. Li,[69] S. Luitz,[69] V. Luth,[69] H. L. Lynch,[69] D. B. MacFarlane,[69] H. Marsiske,[69] R. Messner,[69] D. R. Muller,[69] C. P. O'Grady,[69] V. E. Ozcan,[69] A. Perazzo,[69] M. Perl,[69] T. Pulliam,[69] B. N. Ratcliff,[69] A. Roodman,[69] A. A. Salnikov,[69] R. H. Schindler,[69] J. Schwiening,[69] A. Snyder,[69] J. Stelzer,[69] D. Su,[69] M. K. Sullivan,[69] K. Suzuki,[69] S. K. Swain,[69] J. M. Thompson,[69] J. Va'vra,[69] N. van Bakel,[69] A. P. Wagner,[69] M. Weaver,[69] W. J. Wisniewski,[69] M. Wittgen,[69] D. H. Wright,[69] H. W. Wulsin,[69] A. K. Yarritu,[69] K. Yi,[69] C. C. Young,[69] P. R. Burchat,[70] A. J. Edwards,[70] S. A. Majewski,[70] B. A. Petersen,[70] L. Wilden,[70] S. Ahmed,[71] M. S. Alam,[71] R. Bula,[71] J. A. Ernst,[71] V. Jain,[71] B. Pan,[71] M. A. Saeed,[71] F. R. Wappler,[71] S. B. Zain,[71] W. Bugg,[72] M. Krishnamurthy,[72] S. M. Spanier,[72] R. Eckmann,[73] J. L. Ritchie,[73] C. J. Schilling,[73] R. F. Schwitters,[73] J. M. Izen,[74] X. C. Lou,[74] S. Ye,[74] F. Bianchi,[75] F. Gallo,[75] D. Gamba,[75] M. Pelliccioni,[75] M. Bomben,[76] L. Bosisio,[76] C. Cartaro,[76] F. Cossutti,[76] G. Della Ricca,[76] L. Lanceri,[76] L. Vitale,[76] V. Azzolini,[77] N. Lopez-March,[77] F. Martinez-Vidal,[77] A. Oyanguren,[77] J. Albert,[78] Sw. Banerjee,[78] B. Bhuyan,[78] K. Hamano,[78] R. Kowalewski,[78] I. M. Nugent,[78] J. M. Roney,[78] R. J. Sobie,[78] J. J. Back,[79] P. F. Harrison,[79] T. E. Latham,[79] G. B. Mohanty,[79] M. Pappagallo,[79,§] H. R. Band,[80] X. Chen,[80] S. Dasu,[80] K. T. Flood,[80] J. J. Hollar,[80] P. E. Kutter,[80] B. Mellado,[80] Y. Pan,[80] M. Pierini,[80] R. Prepost,[80] S. L. Wu,[80] Z. Yu,[80] and H. Neal[81]

(*BaBar* Collaboration)

[1]*Laboratoire de Physique des Particules, IN2P3/CNRS et Université de Savoie, F-74941 Annecy-Le-Vieux, France*
[2]*Universitat de Barcelona, Facultat de Fisica, Departament ECM, E-08028 Barcelona, Spain*
[3]*Università di Bari, Dipartimento di Fisica and INFN, I-70126 Bari, Italy*
[4]*Institute of High Energy Physics, Beijing 100039, China*
[5]*University of Bergen, Institute of Physics, N-5007 Bergen, Norway*
[6]*Lawrence Berkeley National Laboratory and University of California, Berkeley, California 94720, USA*
[7]*University of Birmingham, Birmingham, B15 2TT, United Kingdom*
[8]*Ruhr Universität Bochum, Institut für Experimentalphysik 1, D-44780 Bochum, Germany*
[9]*University of Bristol, Bristol BS8 1TL, United Kingdom*
[10]*University of British Columbia, Vancouver, British Columbia, Canada V6T 1Z1*
[11]*Brunel University, Uxbridge, Middlesex UB8 3PH, United Kingdom*
[12]*Budker Institute of Nuclear Physics, Novosibirsk 630090, Russia*
[13]*University of California at Irvine, Irvine, California 92697, USA*
[14]*University of California at Los Angeles, Los Angeles, California 90024, USA*
[15]*University of California at Riverside, Riverside, California 92521, USA*
[16]*University of California at San Diego, La Jolla, California 92093, USA*
[17]*University of California at Santa Barbara, Santa Barbara, California 93106, USA*
[18]*University of California at Santa Cruz, Institute for Particle Physics, Santa Cruz, California 95064, USA*
[19]*California Institute of Technology, Pasadena, California 91125, USA*
[20]*University of Cincinnati, Cincinnati, Ohio 45221, USA*
[21]*University of Colorado, Boulder, Colorado 80309, USA*
[22]*Colorado State University, Fort Collins, Colorado 80523, USA*
[23]*Universität Dortmund, Institut für Physik, D-44221 Dortmund, Germany*
[24]*Technische Universität Dresden, Institut für Kern- und Teilchenphysik, D-01062 Dresden, Germany*
[25]*Laboratoire Leprince-Ringuet, CNRS/IN2P3, Ecole Polytechnique, F-91128 Palaiseau, France*
[26]*University of Edinburgh, Edinburgh EH9 3JZ, United Kingdom*
[27]*Università di Ferrara, Dipartimento di Fisica and INFN, I-44100 Ferrara, Italy*

[28]*Laboratori Nazionali di Frascati dell'INFN, I-00044 Frascati, Italy*
[29]*Università di Genova, Dipartimento di Fisica and INFN, I-16146 Genova, Italy*
[30]*Harvard University, Cambridge, Massachusetts 02138, USA*
[31]*Universität Heidelberg, Physikalisches Institut, Philosophenweg 12, D-69120 Heidelberg, Germany*
[32]*Imperial College London, London, SW7 2AZ, United Kingdom*
[33]*University of Iowa, Iowa City, Iowa 52242, USA*
[34]*Iowa State University, Ames, Iowa 50011-3160, USA*
[35]*Johns Hopkins University, Baltimore, Maryland 21218, USA*
[36]*Universität Karlsruhe, Institut für Experimentelle Kernphysik, D-76021 Karlsruhe, Germany*
[37]*Laboratoire de l'Accélérateur Linéaire, IN2P3/CNRS et Université Paris-Sud 11, Centre Scientifique d'Orsay, B.P. 34, F-91898 ORSAY Cedex, France*
[38]*Lawrence Livermore National Laboratory, Livermore, California 94550, USA*
[39]*University of Liverpool, Liverpool L69 7ZE, United Kingdom*
[40]*Queen Mary, University of London, E1 4NS, United Kingdom*
[41]*University of London, Royal Holloway and Bedford New College, Egham, Surrey TW20 0EX, United Kingdom*
[42]*University of Louisville, Louisville, Kentucky 40292, USA*
[43]*University of Manchester, Manchester M13 9PL, United Kingdom*
[44]*University of Maryland, College Park, Maryland 20742, USA*
[45]*University of Massachusetts, Amherst, Massachusetts 01003, USA*
[46]*Massachusetts Institute of Technology, Laboratory for Nuclear Science, Cambridge, Massachusetts 02139, USA*
[47]*McGill University, Montréal, Québec, Canada H3A 2T8*
[48]*Università di Milano, Dipartimento di Fisica and INFN, I-20133 Milano, Italy*
[49]*University of Mississippi, University, Mississippi 38677, USA*
[50]*Université de Montréal, Physique des Particules, Montréal, Québec, Canada H3C 3J7*
[51]*Mount Holyoke College, South Hadley, Massachusetts 01075, USA*
[52]*Università di Napoli Federico II, Dipartimento di Scienze Fisiche and INFN, I-80126, Napoli, Italy*
[53]*NIKHEF, National Institute for Nuclear Physics and High Energy Physics, NL-1009 DB Amsterdam, The Netherlands*
[54]*University of Notre Dame, Notre Dame, Indiana 46556, USA*
[55]*Ohio State University, Columbus, Ohio 43210, USA*
[56]*University of Oregon, Eugene, Oregon 97403, USA*
[57]*Università di Padova, Dipartimento di Fisica and INFN, I-35131 Padova, Italy*
[58]*Laboratoire de Physique Nucléaire et de Hautes Energies, IN2P3/CNRS, Université Pierre et Marie Curie-Paris6, Université Denis Diderot-Paris7, F-75252 Paris, France*
[59]*University of Pennsylvania, Philadelphia, Pennsylvania 19104, USA*
[60]*Università di Perugia, Dipartimento di Fisica and INFN, I-06100 Perugia, Italy*
[61]*Università di Pisa, Dipartimento di Fisica, Scuola Normale Superiore and INFN, I-56127 Pisa, Italy*
[62]*Prairie View A&M University, Prairie View, Texas 77446, USA*
[63]*Princeton University, Princeton, New Jersey 08544, USA*
[64]*Università di Roma La Sapienza, Dipartimento di Fisica and INFN, I-00185 Roma, Italy*
[65]*Universität Rostock, D-18051 Rostock, Germany*
[66]*Rutherford Appleton Laboratory, Chilton, Didcot, Oxon, OX11 0QX, United Kingdom*
[67]*DSM/Dapnia, CEA/Saclay, F-91191 Gif-sur-Yvette, France*
[68]*University of South Carolina, Columbia, South Carolina 29208, USA*
[69]*Stanford Linear Accelerator Center, Stanford, California 94309, USA*
[70]*Stanford University, Stanford, California 94305-4060, USA*
[71]*State University of New York, Albany, New York 12222, USA*
[72]*University of Tennessee, Knoxville, Tennessee 37996, USA*
[73]*University of Texas at Austin, Austin, Texas 78712, USA*
[74]*University of Texas at Dallas, Richardson, Texas 75083, USA*
[75]*Università di Torino, Dipartimento di Fisica Sperimentale and INFN, I-10125 Torino, Italy*
[76]*Università di Trieste, Dipartimento di Fisica and INFN, I-34127 Trieste, Italy*
[77]*IFIC, Universitat de Valencia-CSIC, E-46071 Valencia, Spain*
[78]*University of Victoria, Victoria, British Columbia, Canada V8W 3P6*
[79]*Department of Physics, University of Warwick, Coventry CV4 7AL, United Kingdom*
[80]*University of Wisconsin, Madison, Wisconsin 53706, USA*

---

[*] Deceased.

[†] Also with Università di Perugia, Dipartimento di Fisica, Perugia, Italy.

[‡] Also with Università della Basilicata, Potenza, Italy.

[§] Also with IPPP, Physics Department, Durham University, Durham DH1 3LE, United Kingdom.

[81]*Yale University, New Haven, Connecticut 06511, USA*

(Received 5 February 2007; published 5 October 2007)

We present a measurement of the time-dependent CP asymmetry for the neutral B-meson decay into the $CP = +1$ final state $K_S^0\pi^0\pi^0$, with $K_S^0 \to \pi^+\pi^-$. We use a sample of approximately 227 million B-meson pairs recorded at the $\Upsilon(4S)$ resonance with the *BABAR* detector at the PEP-II B-Factory at SLAC. From an unbinned maximum likelihood fit, we extract the mixing-induced CP-violation parameter $S = 0.72 \pm 0.71 \pm 0.08$ and the direct CP-violation parameter $C = 0.23 \pm 0.52 \pm 0.13$, where the first uncertainty is statistical and the second systematic.

DOI: 10.1103/PhysRevD.76.071101 PACS numbers: 13.25.Hw, 11.30.Er, 12.15.Hh

CP violation effects in decays of B mesons dominated by $b \to s\bar{q}q$ transitions ($q = u, d, s$) are potentially sensitive to contributions from physics beyond the standard model (SM) [1]. The B-factory experiments have explored time-dependent CP-violating (CPV) asymmetries, occurring due to a phase difference between mixing and decay amplitudes, in several such decays [2], including $B^0 \to \phi K^0$ [3–6], $B^0 \to K_S^0K_S^0K_S^0$ [6,7], $B^0 \to \eta' K_S^0$ [3,5,6,8], $B^0 \to K^+K^-K_S^0$ [3,5,9], $B^0 \to f_0(980)K_S^0$ [5,10], and $B^0 \to K_S^0\pi^0$ [5,11]. Within the SM, the magnitude of the CPV asymmetry in these decays is expected to be approximately equal to the one in $b \to c\bar{c}s$ decays, such as $B^0 \to J/\psi K_S^0$ [1]. A major goal of the B-factory experiments is to reduce the experimental uncertainties of these measurements and to add more decay modes in order to improve the sensitivity to beyond-the-SM effects. In this paper we present a measurement of the CPV asymmetry in the decay $B^0 \to K_S^0\pi^0\pi^0$. The $K_S^0\pi^0\pi^0$ final state is a CP-even eigenstate, regardless of any resonant substructure [12]. In the SM this decay is dominated by the $b \to s\bar{q}q$ weak amplitude, with $q = u, d$, and we expect $S \simeq -\sin 2\beta$ and $C \simeq 0$ [1]. Here C and S are, respectively, the magnitudes of CP violation in the decay and in the interference between decay and mixing, and the angle β is defined as $\beta = \arg(-V_{cd}V_{cb}^*/V_{td}V_{tb}^*)$, where V_{ij} are the elements of the Cabibbo-Kobayashi-Maskawa quark-mixing matrix [13]. A possible contribution from a tree-level $b \to u\bar{u}s$ amplitude is doubly Cabibbo suppressed with respect to the leading gluonic penguin diagram.

The data used in this analysis were collected with the *BABAR* detector [14] at the PEP-II asymmetric-energy e^+e^- collider [15]. A sample of 226.6 ± 2.5 million $B\bar{B}$ pairs was recorded at the $\Upsilon(4S)$ resonance center-of-mass energy $\sqrt{s} = 10.58$ GeV. The *BABAR* detector is described in detail elsewhere [14]. Charged particles are detected and their momenta measured by the combination of a silicon vertex tracker (SVT), consisting of five layers of double-sided detectors, and a 40-layer central drift chamber, both operating in a 1.5 T solenoidal magnetic field. Charged-particle identification is provided by measurements of energy loss in the tracking devices and by an internally reflecting ring-imaging Cherenkov detector covering the central region. Photons are detected by an electromagnetic calorimeter (EMC) composed of 6580 CsI(Tl) crystals. The typical resolution for the π^0 signal in the $\gamma\gamma$ invariant mass spectrum is $\sim 7\ \mathrm{MeV}/c^2$.

We search for $B^0 \to K_S^0\pi^0\pi^0$ decays in neutral B meson candidates selected using charged-particle multiplicity and event topology [16]. We reconstruct $K_S^0 \to \pi^+\pi^-$ candidates from pairs of oppositely charged tracks. The two-track combinations must form a vertex with a χ^2 probability greater than 0.001 and a $\pi^+\pi^-$ invariant mass within $11.2\ \mathrm{MeV}/c^2$ of the K_S^0 mass [17]. We form $\pi^0 \to \gamma\gamma$ candidates from pairs of photon candidates in the EMC, where each photon is isolated from any charged track, carries a minimum energy of 30 MeV, and has the expected lateral shower shape. B meson candidates are formed from $K_S^0\pi^0\pi^0$ combinations and constrained to originate from the e^+e^- interaction region using a geometric fit. We require that the χ^2 probability of the fit is greater than 0.001. We extract the K_S^0 decay length $L_{K_S^0}$ and the $\pi^0 \to \gamma\gamma$ invariant mass from this fit and require $110 < m_{\gamma\gamma} < 160\ \mathrm{MeV}/c^2$ and $L_{K_S^0}$ greater than 5 times its uncertainty. The cosine of the angle between the direction of the decay photons in the center-of-mass system of the mother π^0 and the π^0 flight direction in the lab frame must be less than 0.92.

We reconstruct a B^0 decaying into the CP eigenstate $K_S^0\pi^0\pi^0$ (B_{CP}) and the vertex and flavor of the other B meson (B_{tag}). The difference $\Delta t \equiv t_{CP} - t_{\mathrm{tag}}$ of the proper decay times is obtained from the measured distance between the B_{CP} and B_{tag} decay vertices and from the boost ($\beta\gamma = 0.56$) of the e^+e^- system. Ignoring resolution effects, the Δt distribution is given by

$$\mathcal{P}_{\pm}(\Delta t) = \frac{e^{-|\Delta t|/\tau_{B^0}}}{4\tau_{B^0}}[1 \mp \Delta w \pm (1 - 2w) \times (S\sin(\Delta m_d\Delta t) - C\cos(\Delta m_d\Delta t))]. \quad (1)$$

The upper (lower) sign denotes a decay accompanied by a B^0 ($\bar{B}^0$) tag, τ_{B^0} is the mean neutral B lifetime, Δm_d is the mixing frequency, and the mistag parameters w and Δw are the average and difference, respectively, of the probabilities that a true B^0 is incorrectly tagged as a $\bar{B}^0$ and vice versa. The tagging algorithm [18] has seven mutually exclusive tagging categories of differing purities including one for untagged events that we retain only for yield determinations. The effective tagging efficiency, defined as the tagging efficiency times $(1-2w)^2$ summed over all categories, is $(30.5 \pm 0.6)\%$, as determined from a large sample of B^0-decays to fully reconstructed flavor eigenstates (B_{flav}).

We use the same technique developed for $B^0 \to K_S^0 \pi^0$ decays of Ref. [11] to reconstruct the $B^0 \to K_S^0 \pi^0 \pi^0$ vertex using the knowledge of the K_S^0 trajectory and the average interaction point in a geometric fit [19]. The extraction of Δt has been extensively validated in data [11], and on large samples of simulated $B^0 \to K_S^0 \pi^0 \pi^0$ decays with different values of S and C.

The per-event estimate of the uncertainty on Δt, $\sigma(\Delta t)$, reflects the strong dependence of the Δt resolution on the K_S^0 flight direction and on the number of SVT layers traversed by the K_S^0 decay daughters. In about 70% of the events both pion tracks are reconstructed from at least 4 SVT hits, on either the ϕ or z side, leading to sufficient resolution for the time-dependent measurement. The average Δt event-by-event error, $\sigma_{\Delta t}$, in these events is about 1.0 ps. For events that have fewer than 4 SVT hits or for which $\sigma(\Delta t) > 2.5$ ps or $\Delta t > 20$ ps, the Δt information is not used. However, since C can also be extracted from flavor tagging information alone, these events still contribute to the measurement of C.

We extract the signal yield S and C from an unbinned extended maximum likelihood fit where we parametrize the distributions of several kinematic and topological variables for signal and background events in terms of probability density functions (PDFs).

For each B meson candidate we compute two kinematic variables, the energy difference $\Delta E = E_B^* - \frac{1}{2}\sqrt{s}$ and the beam-energy–substituted mass $m_{\text{ES}} = \sqrt{(\frac{1}{2}s + \vec{p}_0 \cdot \vec{p}_B)^2/E_0^2 - p_B^2}$ [14], where the subscripts 0 and B refer to the initial $\Upsilon(4S)$ and the B_{CP} candidate in the lab frame, respectively, and the asterisk denotes the e^+e^- center-of-mass frame. For signal events, ΔE peaks at zero and m_{ES} at the B meson mass. From a detailed simulation, we expect a signal resolution of about 3.6 MeV$/c^2$ in m_{ES} and 45 MeV in ΔE. Both distributions exhibit a low-side tail due to the response of the EMC to photons. We remove a small dependence of the signal ΔE resolution on the location in the $K_S^0 \pi^0 \pi^0$ Dalitz plot by using $\Delta E/\sigma(\Delta E)$ as a discriminating variable instead of ΔE, where $\sigma(\Delta E)$ is the calculated uncertainty in ΔE. We select candidates with $m_{\text{ES}} > 5.20$ GeV$/c^2$ and $-5 < \Delta E/\sigma(\Delta E) < 2$. To suppress other B meson decays we also require $-0.25 < \Delta E < 0.1$ GeV, which does not affect the signal $\Delta E/\sigma(\Delta E)$ distribution.

The background B meson candidates come primarily from random combinations of K_S^0 and neutral pions produced in continuum events of the type $e^+e^- \to q\bar{q}$, where $q = u, d, s, c$. Background from $B\bar{B}$ events may occur either in charmless decays with a K_S^0 as a decay product, or from decays where the K_S^0 is from an intermediate charmed particle. The shapes of event variable distributions are obtained from signal and background Monte Carlo (MC) samples and high statistics data control samples. The charmless B background forms a broad peak in m_{ES} near the B-meson mass; other B background distributions do not peak in m_{ES}. None of the B backgrounds peak in the $\Delta E/\sigma(\Delta E)$ distribution.

We reduce continuum background events, while retaining 90% of the signal, by requiring $|\cos\theta_T| < 0.9$, where θ_T is the angle between the thrust axis of the B_{CP} candidate's decay products and the thrust axis formed from the other particles in the event. We combine θ_T, the angle between the B_{CP} momentum and the beam axis, θ_B, and the sum of the momenta $\vec{p}_i$ of the other particles in the event weighted by the Legendre polynomials $L_{0,2}(\cos(\theta_i))$ in a neural network (NN). The NN has two hidden layers with 4 neurons each, and is trained and evaluated [20] on different subsets of simulated signal and continuum events and on data taken about 40 MeV below the nominal center-of-mass energy. To parametrize the NN shape, we divide the NN output into intervals, chosen such that they are uniformly populated by signal events (see, e.g., Ref. [21]).

We suppress background from other B decays by excluding several invariant mass intervals: $m(K_S^0\pi^0) > 4.8$ GeV$/c^2$ eliminates $B^0 \to K_S^0\pi^0$, $1.75 < m(K_S^0\pi^0) < 1.99$ GeV$/c^2$ reduces $B^0 \to \bar{D}^0\pi^0$ to fewer than 10 expected candidates, $m(\pi^0\pi^0) < 0.6$ GeV$/c^2$ removes $\eta^{(\prime)}K_S^0$, and $3.2 < m(\pi^0\pi^0) < 3.5$ GeV$/c^2$ removes $\chi_{c0,2}K_S^0$ candidates. The remaining B background comes mainly from $b \to s\gamma$ and $B \to K_S^0\pi^0\pi^0 X$ decays.

The signal reconstruction efficiency after all of the above requirements is about 15%. Based on MC simulations, we expect more than one B_{CP} candidate in 13% of the signal events. The selection of the best candidate is based only on π^0 information, since the number of multiple K_S^0 candidates is negligible (less than 0.1%). We select the candidate whose two π^0 masses $m_{1,2}$ have the least value of $\sum_{i=1}^{2}(m_i - m_{\pi^0})^2$.

For each selected $B^0 \to K_S^0\pi^0\pi^0$ candidate, we examine the remaining tracks in the event to determine the decay vertex position [16] and the flavor of B_{tag} [18]. We parametrize the performance of the tagging algorithm in a data sample of fully reconstructed $B^0 \to D^{(*)-}\pi^+/\rho^+/a_1^+$ decays. For the continuum background, the fraction of events in each tagging category is extracted from a fit to the data.

By exploiting regions in data that are dominated by background, and by using simulated events, we verify that the observables are sufficiently independent that we can construct the likelihood from the product of one-dimensional PDFs, apart from the signal m_{ES} and $\Delta E/\sigma(\Delta E)$ which are correlated. For these observables, we use a two-dimensional PDF derived from a smoothed, simulated distribution. The shape of this distribution is determined by the EMC response, and is validated using π^0s from τ decays and $e^+e^- \to \mu^+\mu^-\gamma$ events. We obtain the PDF for the Δt of signal events from the convolution of Eq. (1) with a resolution function $\mathcal{R}(\delta t \equiv \Delta t - \Delta t_{\mathrm{true}}, \sigma_{\Delta t})$, where Δt_{true} is the actual Δt in the simulated event. The resolution function is parametrized as the sum of two Gaussians with a width proportional to the reconstructed $\sigma_{\Delta t}$, and a third Gaussian with a fixed width of 8 ps that accounts for outliers in the distribution [16]. The first two Gaussian distributions have a nonzero mean, proportional to $\sigma_{\Delta t}$, to account for a bias induced by charm decays on the B_{tag} side. We have verified in simulations that the parameters of $\mathcal{R}(\delta t, \sigma_{\Delta t})$ for $B^0 \to K_S^0 \pi^0 \pi^0$ events are similar to those obtained from the B_{flav} sample, even though the distributions of $\sigma_{\Delta t}$ differ. We therefore extract these parameters from a fit to the B_{flav} sample. We also use this resolution function for the description of background from other charmless B decays. While the resolution functions for B decays into open-charm final states and continuum have the same functional form as used for signal events, the parameters for the Δt PDF of the open-charm background are determined from MC simulation and they are varied in the fit for the continuum.

We subdivide the data into the tagging categories k, events with and without Δt information (sets I and II), and those events located in the inside or outside region of the Dalitz plot (*in* and *out*). The last subdivision accounts for the higher contribution and different characteristics of continuum background near the Dalitz plot boundary. We define the quantity $\delta = \min(m_{12}^2, m_{13}^2, m_{23}^2)$, where m_{ij} is the invariant mass of the B_{CP} decay daughters i and j combined. This δ corresponds to the distance of an event in the Dalitz plot to the nearest Dalitz plot boundary in the limit of massless daughters. We split the data at $\delta = 3.5\ \mathrm{GeV}^2/c^4$.

We maximize the logarithm of the extended likelihood $\mathcal{L} = e^{-(N_S+N_B)} \cdot \prod_{k=1}^{7} \mathcal{L}_k$ with N_S and $N_B = \sum_B n_B$ the total signal and background yields, respectively. The likelihood $\mathcal{L}_k$ in each tagging category k (with tagging fraction ϵ_k) is given as

$$\begin{aligned}\mathcal{L}_k = {} & \prod_j^{N_{\mathrm{I\ out\ k}}} \Big[N_S \epsilon_k^S f_I^S f_{\mathrm{out}}^S P_{k,j}^S + \sum_B n_B \epsilon_k^B f_I^B f_{\mathrm{out}}^B P_{k,\mathrm{out},j}^B \Big] \prod_j^{N_{\mathrm{I\ in\ k}}} \Big[N_S \epsilon_k^S f_I^S (1 - f_{\mathrm{out}}^S) P_{k,j}^S + \sum_B n_B \epsilon_k^B f_I^B (1 - f_{\mathrm{out}}^B) P_{k,\mathrm{in},j}^B \Big] \\ & \times \prod_j^{N_{\mathrm{II\ out\ k}}} \Big[N_S \epsilon_k^S (1 - f_I^S) f_{\mathrm{out}}^S Q_{k,j}^S + \sum_B n_B \epsilon_k^B (1 - f_I^B) f_{\mathrm{out}}^B Q_{k,\mathrm{out},j}^B \Big] \\ & \times \prod_j^{N_{\mathrm{II\ in\ k}}} \Big[N_S \epsilon_k^S (1 - f_I^S)(1 - f_{\mathrm{out}}^S) Q_{k,j}^S + \sum_B n_B \epsilon_k^B (1 - f_I^B)(1 - f_{\mathrm{out}}^B) Q_{k,\mathrm{in},j}^B \Big].\end{aligned}$$

The probabilities P^S (Q^S) and P^B (Q^B) for each measurement j are the products of PDFs for signal (S) and background (B) classes: $P_k = \mathrm{PDF}(m_{\mathrm{ES}}, \Delta E/\sigma(\Delta E))\mathrm{PDF}(\mathrm{NN})\mathrm{PDF}(\Delta t, \sigma(\Delta t), \mathrm{tag}, k)$, where for the background $\mathrm{PDF}(m_{\mathrm{ES}}, \Delta E/\sigma(\Delta E)) = \mathrm{PDF}(m_{\mathrm{ES}})\mathrm{PDF}(\Delta E/\sigma(\Delta E))$. The probabilities Q do not depend on Δt and $\sigma(\Delta t)$ and are used to extract C from the yields. The fractions of events with Δt information for signal and background, f_I^S and f_I^B, and fractions of events in the outside Dalitz plot region, f_{out}^S and f_{out}^B, are varied in the fit except for the fractions for B backgrounds which are determined from simulation. For about 22% of our signal B candidates, one or two of the π^0 decay photons associated with B_{CP} originate from the B_{tag}. According to Monte Carlo simulation studies, we expect to measure the same S and C in these cross-feed events as in the correctly reconstructed signal (*true*) since the contribution of the π^0 to the Δt measurement is marginal. To account for differences in the PDF distributions for the signal probabilities P^S (Q^S), we define the signal probability to be a linear combination of the correctly reconstructed signal and cross-feed events with the relative weight determined from simulation. Parameters of signal PDFs are the same for the different Dalitz plot regions. The PDFs for B backgrounds are identical for the Dalitz inside and outside regions. The tagging fractions for the signal and the B decay backgrounds are the same, while those of the continuum background are different.

The central values of S and C were hidden until the analysis was complete. From a data sample of 33 058 $B^0 \to K_S^0 \pi^0 \pi^0$ candidates, we find $N_S = 117 \pm 27$ signal decays with $S = 0.72 \pm 0.71 \pm 0.08$ and $C = 0.23 \pm 0.52 \pm 0.13$ where the first uncertainty is statistical and the second systematic. There are a total of 30 floating parameters in the fit. The linear correlation coefficient between the two CP parameters is 2%, and the statistical significance of the signal yield is 5.8σ. The yield of charmless B background is consistent with zero, and the fraction of the signal in the outside Dalitz region is 0.78 ± 0.07. Figure 1 shows the distributions of the event variables m_{ES}, $\Delta E/\sigma(\Delta E)$, and *NN* output, and the ratio of the signal likelihood to signal-plus-background likelihood with all variables included. Figure 2 shows the Δt distributions for the B^0- and the $\bar{B}^0$-tagged subsets, and the raw asymmetry $[N_{B^0} - N_{\bar{B}^0}]/[N_{B^0} + N_{\bar{B}^0}]$, where the N_{B^0} ($N_{\bar{B}^0}$) is the number of B^0 ($\bar{B}^0$)-tagged events. In all plots, data are displayed together with the result from the fit after applying a requirement on the ratio of signal likelihood to signal-plus-background likelihood (computed without the variable plotted) to reduce the background.

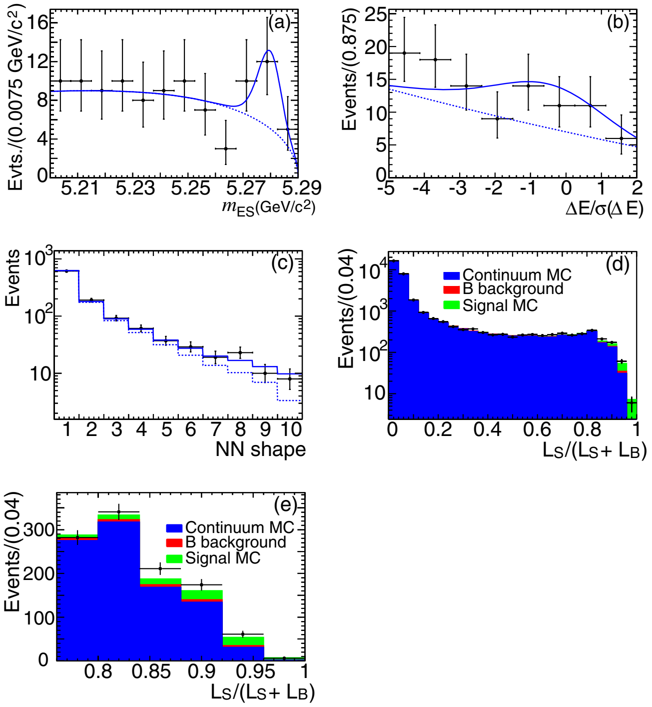

FIG. 1 (color online). Distribution of the event variables (a) m_{ES}, (b) $\Delta E/\sigma(\Delta E)$, and (c) NN output in 10 bins after reconstruction and a requirement on the ratio of signal likelihood to the signal-plus-background likelihood, calculated without the plotted variable. The efficiencies of the likelihood ratio requirements for (a), (b), and (c) are 10%, 26%, and 55%, respectively. The solid line represents the fit result for the total event yield and the dotted line for the total background. Plot (d) shows the ratio of the signal likelihood to signal-plus-background likelihood with all variables included, data (dots) with the fit result superimposed. Plot (e) shows the same quantity as (d) close to 1 and with a linear scale.

We consider the systematic uncertainties listed in Table I. These include the uncertainties in the parametrization of PDFs for signal and backgrounds which were evaluated by varying parameters within 1 standard deviation or using alternative shape functions. The largest contribution to the uncertainty for C is caused by the NN shape for continuum inside the Dalitz plot and for S from the 2D parametrization of m_{ES} and $\Delta E/\sigma(\Delta E)$. We consider uncertainties in the background fractions and *CP* asymmetry in the charmless B background, the parametrization of the Δt resolution function and the vertex finding method, knowledge of the event-by-event beam spot position, imprecision in the SVT alignment, and the possible interference between the suppressed $\bar{b} \to \bar{u}c\bar{d}$ amplitude with the favored $b \to c\bar{u}d$ amplitude for tag-side B-decays [22]. We fix $\tau_{B^0} = 1.532$ ps and $\Delta m_d = 0.505\ \mathrm{ps}^{-1}$ and vary them by 1 standard deviation [17]. We correct for the small fit bias (+ 0.06 on S, and 0.02 on C) which is determined using fits to a large number of simulated experiments, where signal and backgrounds are mixed together in the expected proportions. The uncertainty of the fit bias is accounted for as a systematic error.

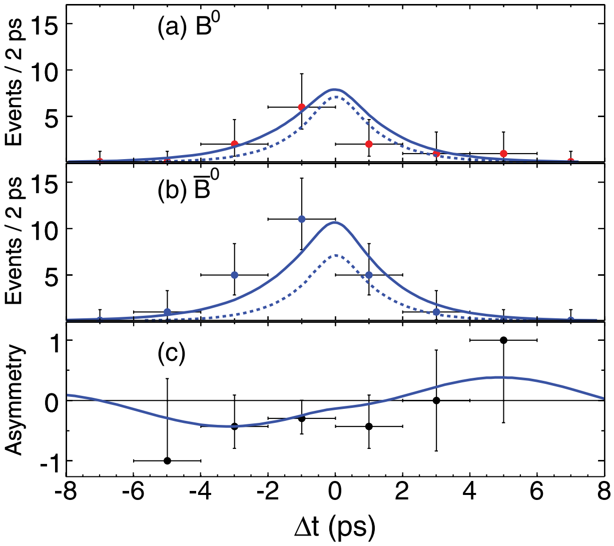

FIG. 2 (color online). Plots (a) and (b) show the Δt distributions of B^0- and $\bar{B}^0$-tagged $B^0 \to K_S^0\pi^0\pi^0$ candidates. The solid lines refer to the fit for all events; the dashed lines correspond to the total background. Plot (c) shows the raw asymmetry (see text). A requirement is applied on the event likelihood to suppress background.

We perform several consistency checks, including the measurement of the B^0 lifetime; we obtain $\tau_{B^0} = 1.25 \pm 0.47$ ps. We embed different B background samples from Monte Carlo simulation in the data sample and obtain consistent yields and *CP* parameters from the fit. We also perform a fit to the data in the $B^0 \to \bar{D}^0\pi^0$ region of the dalitz plot and the yield is consistent with expectations measured branching fractions [17].

In summary, we measure the *CP* violating asymmetries in $B^0 \to K_S^0\pi^0\pi^0$ ($K_S^0 \to \pi^+\pi^-$) decays reconstructed from a sample of approximately 227 million $B\bar{B}$ pairs. From an unbinned extended maximum likelihood fit, we

TABLE I. Sources of systematic uncertainties on S and C. The total error is obtained by summing the individual errors in quadrature.

Source	$\sigma(S)$	$\sigma(C)$
Signal and background PDF parametrization	0.05	0.11
Background fractions	0.03	0.02
CP in charmless B background	0.03	0.01
Vertex finding/resolution function	0.02	0.05
Beam spot position	<0.01	<0.01
SVT alignment	0.02	0.01
Tag-side interference	0.00	0.01
Δm_d, τ_B	0.02	0.01
Fit bias	0.04	0.02
Total systematic error	0.08	0.13

obtain $S = 0.72 \pm 0.71 \pm 0.08$ and $C = 0.23 \pm 0.52 \pm 0.13$. When we fix the values of $-S$ to the average $\sin 2\beta$ measured in $b \rightarrow c\bar{c}s$ modes, $\sin 2\beta = 0.675 \pm 0.026$ [23], and C to zero, and refit the data sample the negative log-likelihood changes by 2.2σ. The signal yield is consistent with our findings in the $B^0 \rightarrow K^0_S\pi^+\pi^-$ decay [24] assuming isospin symmetry and that the dominant charmless final states are $f_0(980)K^0_S$, $K^*(892)\pi^0$, $K^*_0(1430)\pi^0$, and nonresonant $K^0_S\pi^0\pi^0$.

We are grateful for the excellent luminosity and machine conditions provided by our PEP-II colleagues, and for the substantial dedicated effort from the computing organizations that support *BABAR*. The collaborating institutions wish to thank SLAC for its support and kind hospitality. This work is supported by DOE and NSF (U.S.A.), NSERC (Canada), IHEP (China), CEA and CNRS-IN2P3 (France), BMBF and DFG (Germany), INFN (Italy), FOM (The Netherlands), NFR (Norway), MIST (Russia), MEC (Spain), and PPARC (United Kingdom). Individuals have received support from the Marie Curie EIF (European Union) and the A. P. Sloan Foundation.

---

[1] Y. Grossman and M. P. Worah, Phys. Lett. B **395**, 241 (1997); M. Ciuchini, E. Franco, G. Martinelli, A. Masiero, and L. Silvestrini, Phys. Rev. Lett. **79**, 978 (1997); D. London and A. Soni, Phys. Lett. B **407**, 61 (1997); I. Bigi and A. Sanda, Nucl. Phys. **B281**, 41 (1987).
[2] Unless explicitly stated, conjugate decay modes are assumed throughout this paper.
[3] K. Abe *et al.* (Belle Collaboration), Phys. Rev. Lett. **91**, 261602 (2003).
[4] B. Aubert *et al.* (*BABAR* Collaboration), Phys. Rev. Lett. **93**, 071801 (2004).
[5] K.-F. Chen *et al.* (Belle Collaboration), Phys. Rev. D **72**, 012004 (2005).
[6] K.-F. Chen *et al.* (Belle Collaboration), Phys. Rev. Lett. **98**, 031802 (2007).
[7] B. Aubert *et al.* (*BABAR* Collaboration), Phys. Rev. Lett. **95**, 011801 (2005).
[8] B. Aubert *et al.* (*BABAR* Collaboration), Phys. Rev. Lett. **91**, 161801 (2003).
[9] B. Aubert *et al.* (*BABAR* Collaboration), Phys. Rev. Lett. **93**, 181805 (2004).
[10] B. Aubert *et al.* (*BABAR* Collaboration), Phys. Rev. Lett. **94**, 041802 (2005).
[11] B. Aubert *et al.* (*BABAR* Collaboration), Phys. Rev. Lett. **93**, 131805 (2004).
[12] T. Gershon and M. Hazumi, Phys. Lett. B **596**, 163 (2004).
[13] N. Cabibbo, Phys. Rev. Lett. **10**, 531 (1963); M. Kobayashi and T. Maskawa, Prog. Theor. Phys. **49**, 652 (1973).
[14] B. Aubert *et al.* (*BABAR* Collaboration), Nucl. Instrum. Methods Phys. Res., Sect. A **479**, 1 (2002).
[15] PEP-II Conceptual Design Report, SLAC-R-418, 1993.
[16] B. Aubert *et al.* (*BABAR* Collaboration), Phys. Rev. D **66**, 032003 (2002).
[17] S. Eidelmann *et al.* (Particle Data Group), Phys. Lett. B **592**, 1 (2004).
[18] B. Aubert *et al.* (*BABAR* Collaboration), Phys. Rev. Lett. **94**, 161803 (2005).
[19] W. D. Hulsbergen, Nucl. Instrum. Methods Phys. Res., Sect. A **552**, 566 (2005).
[20] C. G. Broyden, J. Inst. Math. Appl. **6**, 222 (1970); R. Fletcher, Computer Journal **13**, 317 (1970); D. Goldfarb, Math. Comput. **24**, 23 (1970); D. F. Shanno, Math. Comput. **24**, 647 (1970).
[21] B. Aubert *et al.* (*BABAR* Collaboration), Phys. Rev. Lett. **94**, 181802 (2005).
[22] O. Long, M. Baak, R. N. Cahn, and D. Kirkby, Phys. Rev. D **68**, 034010 (2003).
[23] E. Barberio *et al.* (Heavy Flavor Averaging Group), arXiv:hep-ex/0603003, http://www.slac.stanford.edu/xorg/hfag/.
[24] B. Aubert *et al.* (*BABAR* Collaboration), Phys. Rev. D **73**, 031101 (2006).